EFDA–JET–CP(12)02/35

D. Harting, M. Groth, M. Beurskens, P. Boerner, M. Brix, J.W. Coenen,
G. Corrigan, M. Lehnen, S. Marsen, G. van Rooij, D. Reiter, S. Wiesen
and JET EFDA contributors

Simulation of Tungsten Sputtering with EDGE2D-EIRENE in Low Triangularity L-Mode JET ITER-Like Wall Configuration

Simulation of Tungsten Sputtering with EDGE2D-EIRENE in Low Triangularity L-Mode JET ITER-Like Wall Configuration

D. Harting[1], M. Groth[2], M. Beurskens[3], P. Boerner[1], M. Brix[3], J.W. Coenen[1], G. Corrigan[3], M. Lehnen[1], S. Marsen[4], G. van Rooij[5], D. Reiter[1], S. Wiesen[1] and JET EFDA contributors*

JET-EFDA, Culham Science Centre, OX14 3DB, Abingdon, UK

[1]Institut für Energie- und Klimaforschung –IEK-4, Plasmaphysik, Forschungszentrum Jülich, TEC, Association EURATOM-FZJ, D-52425 Jülich, Germany
[2]Aalto University, Association EURATOM-Tekes, Otakaari 4, 02015 Espoo, Finland
[3]EURATOM-CCFE Fusion Association, Culham Science Centre, OX14 3DB, Abingdon, OXON, UK
[4]Max-Planck Institut für Plasmaphysik, Association EURATOM, D-17491 Greifswald, Germany
[5]FOM Institute for Plasma Physics, Rijnhuizen PO Box 1207, 3420BE Nieuwegein, Netherlands
** See annex of F. Romanelli et al, "Overview of JET Results", (23rd IAEA Fusion Energy Conference, Daejon, Republic of Korea (2010)).*

Preprint of Paper to be submitted for publication in Proceedings of the 20th International Conference on Plasma Surface Interactions , Eurogress, Aachen, Germany 21st May 2012 - 25th May 2012

ABSTRACT

The 2D edge plasma transport code EDGE2D-EIRENE [1][2][3] has been upgraded to account for the actual material and geometric properties of the newly installed ITER like wall [4] (ILW) at JET. This includes the simulation of beryllium and tungsten impurities as well as a revised treatment of sputtering by main plasma and impurity atoms and ions (including self sputtering). In this work, two L-mode density regimes, a sheath limited and a high recycling regime, are presented with a power scan from 2 to 6MW. Tungsten is self consistently simulated with the Scrape Off Layer (SOL) plasma by the EDGE2D-EIRENE code. A detailed analysis of the tungsten sputtering is presented, resolving the individual contributions of the different atomic and ion species in the simulations.

1. INTRODUCTION

With the newly developed ILW model for the EDGE2D-EIRENE code, the selfconsistent modelling of tungsten sputtering with the SOL plasma is now available. In this work, the sputtering contribution of the individual plasma species, like atoms and ions of deuterium, beryllium and tungsten are analysed for a sheath-limited and a high-recycling regime. The input power is varied from 2 to 6MW, and the dependence of the tungsten sputtering is presented. It turns out that in the high-recycling regime the tungsten sputtering is dominated by neutral deuterium atoms and beryllium ions. The first section describes the new ILW model and a revised treatment of the tungsten sputtering in the EDGE2D-EIRENE code. The next sections focus on the simulations, describing boundary conditions and main chamber beryllium sputtering. Finally a detailed analysis of the tungsten sputtering in the divertor is presented.

2. REVISED ITER LIKE WALL MODEL IN EDGE2D-EIRENE

Upgrading of the EDGE2D-EIRENE code to account for the actual material and geometrical properties of the new ILW at JET revealed that several key processes for tungsten and beryllium sputtering were not taken into account. This included the ability of impurity ions to sputter the wall material and missing sputtering yields for beryllium on tungsten and vice versa. Beside the sputtering model, also the geometrical representation of the divertor and main chamber wall needed to be revised, to accurately treat the two different wall materials of the ITER like wall.

The EDGE2D code distinguishes between non-recycling and recycling impurities. Recycling impurities (like argon and neon) are recycled at the wall with a recycling coefficient of unity (full recycling). These impurity ion loss fluxes from the EDGE2D domain are passed to EIRENE; as in previous versions of the code, these fluxes have the ability to sputter the wall material. For non-recycling impurities (like carbon, tungsten and beryllium) EDGE2D treats the impurity ion fluxes to the wall as being completely lost (no recycling). In that previous version of the code, the non-recycling impurity ion loss fluxes from the EDGE2D domain were not passed to EIRENE and therefore could not contribute to the sputtering which is simulated on the EIRENE side. The EDGE2D code is now extended to pass also the parallel target fluxes of non-recycling impurity ions to EIRENE where they are accelerated in the sheath and sputter the divertor material. The

perpendicular radial loss fluxes of non-recycling impurity ions are neutralized on the radial EDGE2D boundary (without acceleration in the sheath) and travel radially outwards in an assumed vacuum region towards the main chamber wall where they can also sputter. This new feature is not only necessary for simulations of the ITER like wall, it also includes self-sputtering by carbon ions for the old carbon wall at JET, which was omitted so far in previous EDGE2D-EIRENE versions.

In the sputtering model of EIRENE, the physical sputtering yield is calculated by the revised Bohdansky formula (eq. 10 in [5]). The coefficients for this revised Bohdansky formula are taken from table 3 in [5] which provides experimentally optimised coefficients for several target/projectile combinations. However, the projectile/target combinations beryllium/tungsten and tungsten/beryllium are not included in table 3 of [5] which resulted in a sputtering yield of zero for these material combinations. The sputtering model of the latest EIRENE version solves this problem by applying empirical formulas (eq. 7, 27, 28 in [5]) to calculate the coefficients for the revised Bohdansky formula where the projectile/target material combinations are missing in table 3 of [5]. This new physical sputtering model of EIRENE is now also included in the EIRENE version used by EDGE2D, which enables EDGE2D-EIRENE to treat physical sputtering on the ILW accurately.

The ILW material changes from a tungsten divertor to a beryllium main chamber on top of the inner and outer divertor shoulders. However the old wall model of the EDGE2DEIRENE code defined the tungsten divertor by the region covered from the inner to the outer divertor targets of the EDGE2D grid (inner target, private wall and outer target in figure 1). This could lead, especially for horizontal target configurations (outer strike point on tile 5 [6]), to an assumed full beryllium outer vertical divertor in the EDGE2D-EIRENE simulation, which overestimates the beryllium production in the divertor. For this reason the wall model of the EDGE2D-EIRENE interface was extended to allow for multiple wall materials in the void region to cover the full inner and outer vertical part of the tungsten divertor. This facilitates now the EDGE2D-EIRENE code to use the actual experimental situation where the material of the ILW changes from a tungsten divertor to the beryllium main chamber wall (figure 1).

3. EDGE2D-EIRENE SIMULATIONS OF TUNGSTEN SPUTTERING WITH THE ILW AT JET

3.1 SETUP OF SIMULATIONS

Utilising the experimental data at the outer midplane, the 2-D multi-fluid edge code EDGE2D coupled to the neutral kinetic Monte Carlo code EIRENE was exercised to predict the same divertor parameters as obtained experimentally [7]. All simulations presented here were executed on a common grid, reflecting the low triangularity configuration of Pulse No: 81472 at 50s. In EDGE2D, plasma transport in the parallel-B direction is modelled using the Braginskii equations; here, flux limiters were not applied. Two impurities (beryllium and tungsten) are modelled as individual fluids in thermal equilibrium with the main plasma ($T_{imp} = T_{main\ plasma}$), and bundling of tungsten in six charge states was imposed to enable tungsten transport calculations[8]. In the radial direction, a purely diffusive model with radially varying (effective) transport coefficients was assumed. The

physics of cross-field drifts (**E×B** and **B×∇B**) are not included in these simulations. To match the measured upstream profiles for n_e, T_e, and T_i at the outer midplane, particle diffusion coefficients of $1.0 m^2/s$ were applied in the core region up to the pedestal (at $R-R_{sep,OMP}$ of $-1cm$, where Rsep,OMP is the radial position of the separatrix at the Outer MidPlane (OMP)), $0.5 m^2/s$ in the pedestal and near-separatrix region ($-1cm < R-R_{sep,OMP} < 1cm$), and $1.0 m^2/s$ in the mid and far SOL. These parameters represent a fair match to the experimental profiles with an separatrix density of $n_{sep,OMP} = 0.8\times10^{19}\ m^{-3}$ [7]. A step function was assumed for both the ion and electron thermal diffusivities in the radial direction: $1.0 m^2/s$ in the core and pedestal region, and $0.5 m^2/s$ in the SOL. These settings were found to produce a sufficient match to the experimental T_e profile at the OMP [7].

Fuelling and pumping of deuterium atoms and molecules as well as beryllium and tungsten atoms, and their transport within the plasma, are simulated with EIRENE. The injection and pump locations were adapted as in the experiment, where deuterium molecules are injected in the divertor region and removed in the corners of the divertor. Pump albedos of 0.94 were assumed. Along all beryllium and tungsten ILW elements, deuterium neutrals and ions are recycled as atoms or molecules calculated by TRIM [9][10]. Impurities are self consistently generated by physical sputtering[11] due to neutral and ion impact at the target plates, including tungsten and beryllium self-sputtering. In the main chamber and private region, only neutrals (D, Be, W) sputter impurities.

Two different SOL density regimes, a sheath limited with a separatrix density of $n_{sep,OMP} = 0.5\times10^{19}\ m^{-3}$ and a high recycling with $n_{sep,OMP} = 1.0\times10^{19}\ m^{-3}$, around the experimental separatrix density of $n_{sep,OMP} = 0.8\times10^{19}\ m^{-3}$ were chosen to investigate the tungsten sputtering in the simulation. For both densities regimes the input power entering the SOL from the core was ramped from 2.0MW to 6.0MW in nine steps, equally distributed between electrons and ions. For each of the power steps a fully converged solution was obtained, and the contribution of the individual atomic and ion species to the tungsten and beryllium sputtering is analysed.

3.2 MAIN CHAMBER SPUTTERING OF BERYLLIUM

Sputtering on the main chamber wall by neutral particles is the only source for beryllium impurities in the simulation. This represents a lower limit, because if ions would reach the beryllium wall more beryllium would be sputtered. The total sputtered beryllium flux rises nearly linearly from $2.8\times10^{20}\ s^{-1}$ to $3.9\times10^{20}\ s^{-1}$ for the sheath limited case ($n_{sep} = 0.5\times10^{19}\ m^{-3}$) and from $4.2\times10^{20}\ s^{-1}$ to $5.9\times10^{20}\ s^{-1}$ for the high-recycling case ($n_{sep} = 1.0\times10^{19}\ m^{-3}$) with increasing input power between 2 and 6 MW. Due to the low sputtering threshold of beryllium (regarding projectile energies) and the dominant influx of deuterium atoms (more than a factor of 100 higher than the atomic impurity influx) practically 100% of the beryllium is sputtered by deuterium atoms with an effective sputtering yield of 3% for the sheath limited and 2% for the high-recycling case. This leads to a roughly constant beryllium content of about 1% compared to the deuterium content in the SOL (figure 2). For similar conditions, a beryllium content of 0.5% was estimated experimentally[12].

3.3 DIVERTOR SPUTTERING OF TUNGSTEN

The behaviour of tungsten sputtering in the divertor is more complex than the beryllium main

chamber sputtering. For the analysis we distinguish between 4 regions of the tungsten divertor wall, which are defined by the magnetic configuration of the EDGE2D grid.

The inner and outer target regions (figure 1) are wetted by parallel ion influxes around the strike points plus incoming neutral particle fluxes, and the outer vertical divertor and private wall regions (figure 1) can only be reached by radially outwards diffusing neutral particles. The total sputtered tungsten flux for the sheath limited regime rises from $1.8\times10^{19}\ s^{-1}$ to $5.6\times10^{20}\ s^{-1}$ with increasing input power. Regarding the resulting separatrix ion temperatures (see figure 3) one must bear in mind that the plasma would be well in H-mode for heating powers above 4MW (ion target temperatures > 180eV) in the sheath limited regime, which is disregarded in the simulation. Due to the much lower plasma temperatures in the high recycling regime (figure 3), the tungsten sputtering is drastically reduced by an order of magnitude, and the total sputtered tungsten flux rises only from $2.4\times10^{18}\ s^{-1}$ to $2.4\times10^{19}\ s^{-1}$ during the power ramp. This is also reflected in the tungsten content (figure 2), which in the high recycling regime is also reduced nearly by an order of magnitude compared to the sheath-limited regime.

Regarding the individual species contributions to the total sputtered tungsten flux, it turns out that especially for low ion target temperatures, neutral deuterium atoms sputter up to 65% of the total sputtered tungsten (figure 4). This is facilitated by Charge eXchange (CX) processes between the neutral deuterium atoms and higher energetic deuterium ions inside the plasma, which increase the high-energy tail of the velocity distribution of the neutral deuterium atoms. These high energetic deuterium atoms can exceed the sputtering threshold of tungsten, and thereby dominate the sputtering. Due to the high temperature target conditions of the sheath-limited regime (figure 4, right), still a significant fraction (10-40%) of the tungsten is sputtered by beryllium ions. Even though the tungsten flux sputtered by beryllium ions and deuterium atoms still increases with higher input powers, their contribution to the total sputtered tungsten decreases, as the self sputtering of tungsten by tungsten ions becomes the dominant part for ion target temperatures above 170eV. The contribution of the neutral tungsten and beryllium atoms to the tungsten sputtering can be neglected, as charge exchange processes for these impurity atoms are not included in the simulations. This is a fair assumption, as due to their low ionization energies, the neutral impurities do not penetrate as deep as the deuterium in to the hot plasma, and their neutral atom densities are more than two orders of magnitude lower than the deuterium atom density.

In the high recycling regime (see figure 4, left), the tungsten sputtering is mostly dominated by sputtering due to neutral deuterium atoms. Only for ion target temperatures below 10eV the beryllium ions have a large contribution of about 50% to the total tungsten sputtering, but their fraction decreases down to 15% with increasing ion target temperatures. Deuterium and tungsten ions barely contribute to the tungsten sputtering (<1%) for ion target temperatures below 40eV. Only for ion target temperatures above 50eV their contribution raises up to 15% with increasing ion target temperatures, as tungsten ions exceeds their selfsputtering threshold of approximately 70eV. Also the deuterium ion contributions raises already from ion target temperatures around 50eV, as their ion influx is up to 4 orders of magnitude higher than the tungsten ion influx on the targets, and

therefore still a significant fraction from the high energy Maxwell tail can exceed the deuterium threshold of about 250eV for tungsten sputtering.

Analysing different areas of the tungsten divertor for the high-recycling regime, the simulations show that 50-60% of the total sputtered tungsten comes from the inner vertical target (solid fluxtot in figure 5). Another 40% is sputtered at the outer target and outer vertical divertor (dashed fluxtot in figure 5). The private wall region between the inner and outer target regions (see figure 1) contributes less than 10% to the total sputtered tungsten flux, and is neglected in the further analysis. Regarding the individual contributions of the different species to the tungsten sputtering on the inner divertor target (solid lines in figure 5), it turns out that beryllium ions are the dominant species. Their contribution decreases from 90% to 30% with increasing ion target temperatures. At the same time, the contribution of the neutral deuterium atoms raises from 10% to 40% at the inner targets. In contrast to that, the tungsten sputtering at the outer target and outer vertical divertor is completely dominated by the neutral deuterium atoms (dashed lines in figure 5). The different behaviour at the inner and outer divertor comes from the fact that the density of beryllium ions is about a factor of 10 higher near the inner vertical divertor than at the outer divertor. For the neutral deuterium atoms it is the other way around. Their density is about a factor of 10 higher at the outer divertor compared to the inner vertical divertor.

CONCLUSIONS

EDGE2D-EIRENE simulations with an upgraded sputtering model for impurities show that the species contribution to the tungsten sputtering have similar trends for the high recycling and the sheath limited cases in the simulations, just for different ion target temperature regimes. Due to the low ion target temperatures in the high recycling regime, tungsten self-sputtering is nearly absent and contributes only significantly to the sputtering in the sheath-limited regime. Surprisingly, the neutral deuterium atoms play an important role in the tungsten sputtering. Due to charge exchange processes with hot plasma ions from radially further inside, the high-energy tail of the velocity distribution of the deuterium atoms is increased and they can exceed the sputtering threshold of tungsten. This leads to a contribution to the tungsten sputtering of 15% to 50% for the sheath limited and 40% to 65% in the high recycling regimes, depending on the actual ion target temperatures.

ACKNOWLEDGEMENT

This work, supported by the European Communities under the contract of Association between EURATOM and FZ-Jülich, was carried out within the framework of the European Fusion Development Agreement. The views and opinions expressed herein do not necessarily reflect those of the European Commission.

REFERENCES:

[1]. R. Simonini, G. Corrigan et al., Contribution to Plasma Physics **34** 2/3 (1994) 368-373.

[2]. S. Wiesen, www.eirene.de/e2deir_report_30jun06.pdf

[3]. www.eirene.de
[4]. G.F. Matthews et al., Physica Scripta **2011** (2011) 014001.
[5]. W. Eckstein, C. Garcia-Rosales, J. Roth, et al. „Sputtering Data“, MPI-Garching Report **IPP-9/82**, MPI-Garching, February 1993.
[6]. S. Brezinsek et al., Journal of Nuclear Materials **415** (2011) S936.
[7]. M. Groth et al., “Target particle and heat loads in low-triangularity L-mode plasmas in JET with carbon and beryllium/tungsten walls”, this conference.
[8]. J.D. Strachan, G. Corrigan, D. Harting et al., “EDGE2D comparisons of JET tungsten and carbon screening”, Journal of Nuclear Materials **415** 1 (2011), S501-S504.
[9]. W. Eckstein and D.B. Heifetz. “Data sets for hydrogen reflection and their use in neutral transport calculations”. MPI-Garching Report **IPP-9/59**, MPI-Garching, August 1986. Journal of Nuclear Materials **145-147** (1987), p332.
[10]. G. Bateman, “Distribution of neutrals scattered off a wall” PPPL Applied Physics Repeport No. **1**, PPPL, 1980.
[11]. W. Eckstein, Journal of Nuclear Materials **248** (1997) 1.
[12]. G. van Rooij et al., this conference.

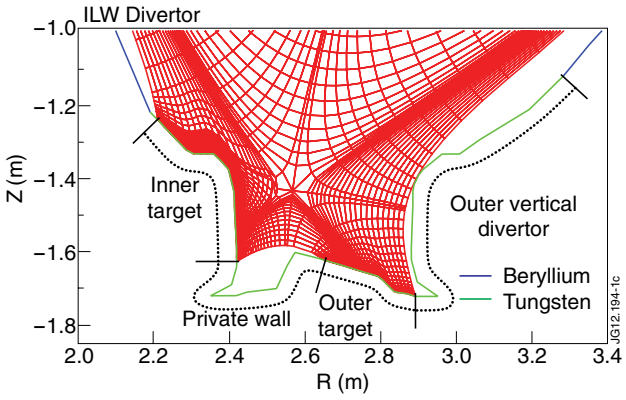

Figure 1: Regions in the ILW divertor with beryllium representing actual main chamber surfaces and tungsten divertor surfaces.

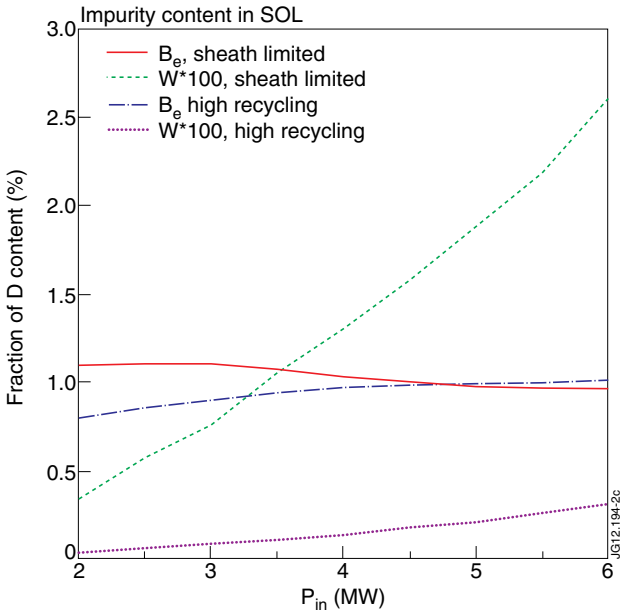

Figure 2: Fraction of beryllium and tungsten content with increasing input power P_{IN} compared to the deuterium main plasma content in the SOL of about 5×10^{19} particles for the sheath limited and 7×10^{19} particles for high recycling regime. The tungsten content in this figure is scaled by a factor of 100 to display in the same scale with the beryllium content.

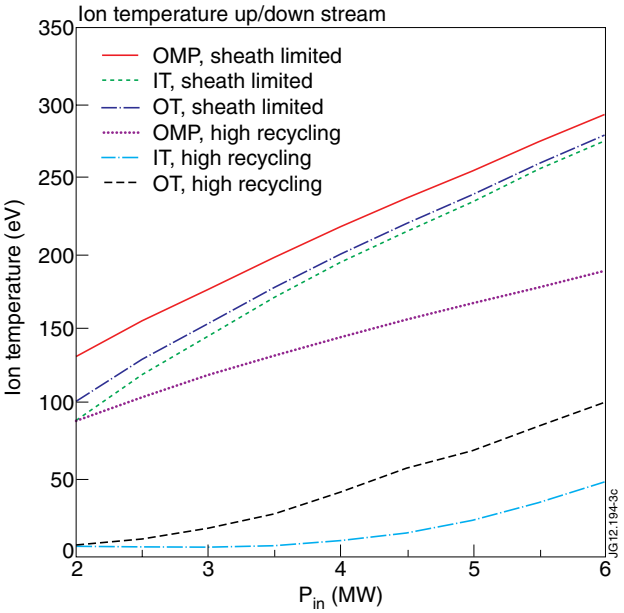

Figure 3: Ion temperatures at the separatrix (OMP) and at the Inner Target (IT) and Outer Target (OT) for both density regimes of the simulations.

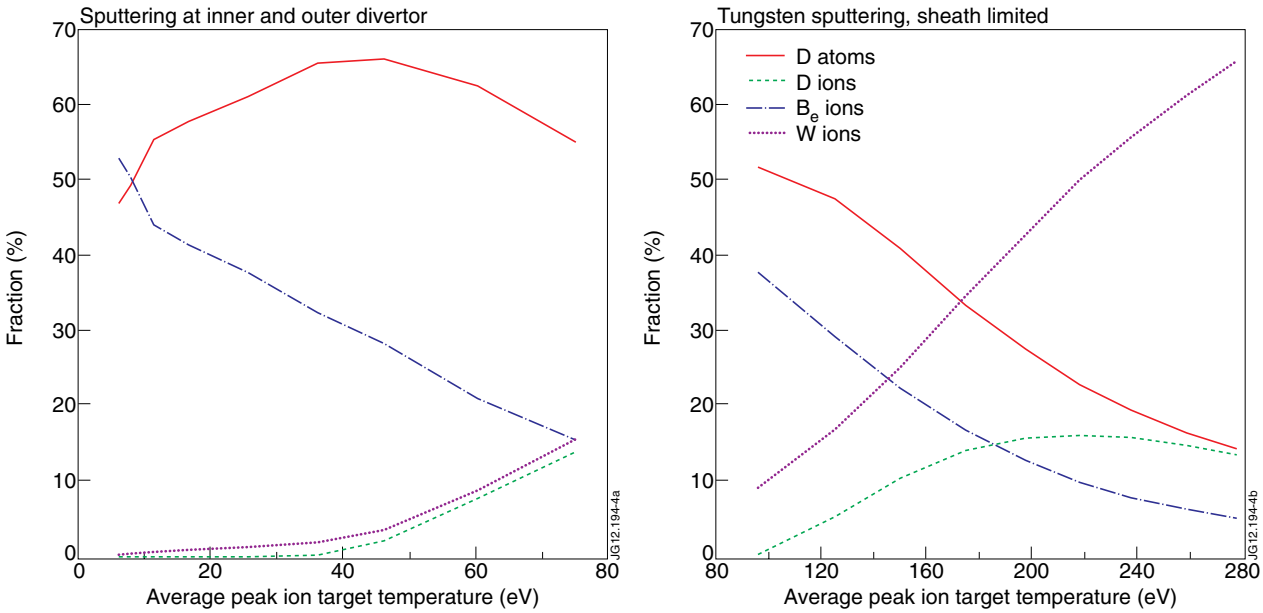

Figure 4: Relative contribution to the total tungsten sputtering of each individual species for the high recycling (left) and sheath limited (right) regime. Average ion target temperatures represent input powers between 2 and 6MW for both regimes.

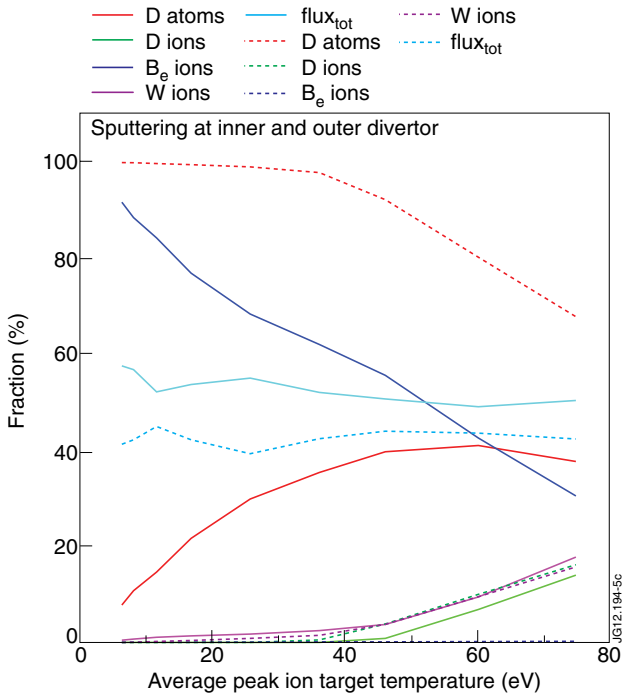

Figure 5: Relative contribution to the tungsten sputtered from the inner vertical target (solid lines) and the outer target and outer vertical divertor (dashed lines) of each individual species in the high recycling regime. Additionally also the fraction of the tungsten sputtered from each of the regions compared to the total sputtered tungsten is shown (fluxtot).